doi.org/10.52568/001071/JCSP/44.04.2022

Metabolomic Profiling of Different Maca Color Types Using Nuclear Magnetic Resonance Spectroscopy and Multivariate Data Analysis

Jingwei Lv, Chunnan Li, Nanxi Zhang, Kaiyue Zhang, Xiaochen Gao, Na Li, Lingwen Meng, Yinping Yang, Hui Zhang* and Jiaming Sun*

Jilin Ginseng Academy, Changchun University of Chinese Medicine, Changchun 130117, China.

sun_jiaming2000@163.com*

(Received on 22 January 2021, accepted in revised form 9th December 2021)

Summary. This study aimed to explore significant differences in chemical composition among maca (*Lepidium meyenii* Walp.) types with different colors in Yunnan province, China. ^{1}H-NMR spectroscopy, in combination with principal component analysis and partial least squares discriminant analysis, was used to investigate the compounds responsible for compositional differences. Different maca color types in Yunnan were clearly distinguished by 11 differential metabolites. Furthermore, network pharmacology results showed that 30 active components were related to Alzheimer's disease. Nine intersecting compounds among the 11 differential metabolites and 30 active components, namely, lysine, isoleucine, phenylalanine, β-hydroxybutyrate, tryptophan, pyroglutamate, proline, glutamine, and fructose, were used as bioactive markers to identify different maca color types. The results showed the bioactive markers among different maca color types holistically, providing a scientific basis for assessing the quality of commercial products derived from different maca color types.

Keywords: ^{1}H-NMR spectroscopy; Multivariate data analysis; Maca; Metabolomic.

Introduction

Maca (*Lepidium meyenii* Walp.), a Peruvian plant from the Brassicaceae family [1], grows in the Central Andean Region between altitudes of 3800 and 4800 m. Since 2002, maca has been successfully transplanted to the Chinese provinces of Yunnan, Sichuan and Xinjiang, resulting in large-scale planting [2]. Maca grown at high altitudes is rich in sugar, fat, and protein, providing nourishment to humans and animals. Maca, among other plants, is traditionally employed to improve sexuality and fertility. Studies have shown that maca has many health-related properties, including beneficial effects on fertility, memory, osteoporosis and skin [3-9]. Therefore, maca has been planted in Asia and North America, and global consumption is increasing. Recently, studies have shown that the main active ingredients of maca are macamide, macaene, and maca glucosinolates, among others [10, 11]. Presently, maca is used not only to treat diseases such as diarrhea, rheumatism, and breathing, but also to regulate hormone secretion, promote metabolism, enhance memory, as an antidepressant, and to treat anemia, leukemia, AIDS, and cancer, among other applications [12-17]. Maca has extensive market development and application prospects.

Maca is rich in amino acids, glucose, fat, and other nutrients, and also contains various secondary metabolites, such as macamide, glycogen, sterol, and polyphenols [18-20]. The composition of maca is complex because its components are influenced by geographical and environmental conditions, such as altitude and dimensions, with the compositions of different polar chemical components showing obvious regional changes. Therefore, traditional quantitative analysis methods cannot be relied upon to evaluate the quality characteristics of maca, with a holistic approach needed. Metabonomics is the branch of science concerned with quantitatively understanding the metabolite complement of integrated living systems and its dynamic response to changes in both endogenous factors (such as developmental physiology) and exogenous factors (such as environmental factors and xenobiotics) [21]. Metabonomics aims to understand the physiological and pathological state of an organism through the comprehensive analysis of metabolites with low relative molecular weights after exposure to external stimuli. Presently, metabonomics is widely used in studies on traditional Chinese medicine (TCM), providing strong technical support for the safety evaluation of TCM, the material basis and mechanisms of Chinese medicinal formulas, and understanding the recognition of TCM syndromes and signs [22]. Its application in combination with chemometrics methods can be used to analyze complex systems, such as TCM chemical composition and corresponding activity, to achieve rapid screening of active ingredients. Network pharmacology is now considered to be a holistic and efficient tool for studying the role of TCM. Accordingly, an integrated model combining disease target prediction and compounds from the molecular network level was developed to explain the mechanism of action of herbal compounding [23]. To our knowledge, the use of ^{1}H-NMR spectroscopy to quantify metabolites to determine the major water-soluble low-molecular-weight components in maca has rarely been reported [24].

In this study, compositional differences in maca

*To whom all correspondence should be addressed.

types with different colors were determined and combined with multivariate statistical analysis. The relationship between differential metabolites and the inner quality of maca was studied in depth, providing a basis for the evaluation of maca quality characteristics.

Experimental

Materials, solvents, and chemicals

Maca bodies were collected in November 2017, from sites representing macro habitats in Lijiang County, Yunnan Province, China. For different maca color types, 40 fresh annual samples were collected and authenticated by Prof. Hui Zhang of the Changchun University of Chinese Medicine. Clean the fresh maca, cut off the bottom of the stem, and remove the attached matrix fragments. The samples were air-dried using a desiccator at 40 ℃ for 72 h. Maca root was generally dried, powdered, and stored in Celine bottles. All specimens are preserved in the herbarium of Changchun University of Chinese Medicine, China.

Analytical grade methanol and trichloromethane were obtained from Beijing Chemical Works (Beijing, China). Sodium 3-trimethylsilyl [2, 2, 3, 3-d4] propionate (TSP) was obtained from Cambridge Isotope Laboratories Inc. (Andover, MA, USA). Analytical grade $Na_2HPO_4 \cdot 12H_2O$ and analytical grade $NaH_2PO_4 \cdot 2H_2O$ were obtained from Beijing Chemical Works (Beijing, China). Cell culture reagents, penicillin–streptomycin solution, trypsin-EDTA, and fetal bovine serum (FBS) were obtained from Gibico Co. (California, USA). Culture flasks were acquired from Corning Co. (New York, USA). The 3-[4,5-Dimethyl-2-thiazolyl]-2,5-diphenyl-2-tetrazolium bromide (MTT) (Sigma, Saint Louis, MO, USA). L-Glutamic acid was obtained from Aladdin Co. (California, USA).

Cell viability analysis

Human neuroblastoma SH-SY5Y cells were obtained from Shanghai Cell Bank, Chinese Academy of Medical Sciences (Shanghai, China). Cells were grown with MEM medium supplemented with 10% fetal bovine serum and maintained at 37 °C in a 5% CO_2 atmosphere. After two passages, it was incubated at a density of 4,000 per well in a 96-well microplate. The cells were then incubated with L-glutamic acid (5 mM) and different concentrations of maca for 24 h. Maca was added 30 min before L-glutamic acid. Cell viability was detected by absorbance (OD) value at 490 nm by the MTT method and repeated six times. The results are expressed as percentages of the control values.

Sample preparation for ^{1}H-NMR analysis

For different maca color types, a two-phase extraction method comprising MeOH–H_2O in a 1:2 (v/v) ratio (MeOH, 3 mL; H_2O, 6 mL) was used to extract the metabolites from pulverized maca samples with different colors (1 mg) in a 50 mL centrifuge tube. The sample was broken by intermittent ultrasound for 20 minutes, centrifuged at 13 000 rpm for 10 minutes, the supernatant (510 μL), 0.05%TSP (30 μL) and D2O (60 μL) were transferred into a 5 mm NMR tube for ^{1}H-NMR analysis.

^{1}H-NMR measurements

^{1}H-NMR analysis was conducted at 25 ℃ on a Bruker 600-MHz AVANCE III NMR spectrometer (Bruker, Karlsruhe, Germany) operating at a ^{1}H-NMR frequency of 600 MHz. The ^{1}H-NMR spectra used the standard NOESYPRGP1D pulse sequence. A waiting time of 3 s and a mixing time of 300 ms were used for the low-power continuous wave pulse for water peak suppression. TSP was used as internal standard. Each ^{1}H-NMR spectra consisted of 64 scans, requiring 5-min acquisition times with the following parameters: 0.18 Hz/point; pulse width (PW), 5498.53 Hz at 90° (12.08 μs); sampling time, 1.86 s; and relaxation delay (RD), 5.0s [25].

Data analysis

The as-obtained ^{1}H-NMR spectra were processed using MestReNova software (version 5.2.5, Mestrelab Research, Santiago de Compostella. Spain). After positioning, baseline calibration, and normalization, the nuclear magnetic spectrum δ 0.0 ~ 9.0 area δ 0.04 interval piecewise integral, where δ 4.80 ~ 5.06 (residual water peak) shall not be integrated, and the integrated data shall be imported into excel table for sorting. The obtained data were imported into SIMCA-P 14.1 software (Umetrics, Umeå, Sweden) for multivariate statistical analysis, including principal component analysis (PCA) and partial least squares discriminant analysis (PLS-DA).

Construction a target-metabolite network

A list of differential metabolites that were derived from the experimental part of the study was used as the input data for the MetScape tool [26]. Subsequently, key targets involved in AD were obtained from the TTD database (http://db.idrblab.net/ttd/). According to the network constructed by MetScape, the potential interactions between the metabolites and targets were obtained. A bio-network of target-metabolite was constructed using Cytoscape3.7.2 (http://www.cytoscape.org/) software [27].

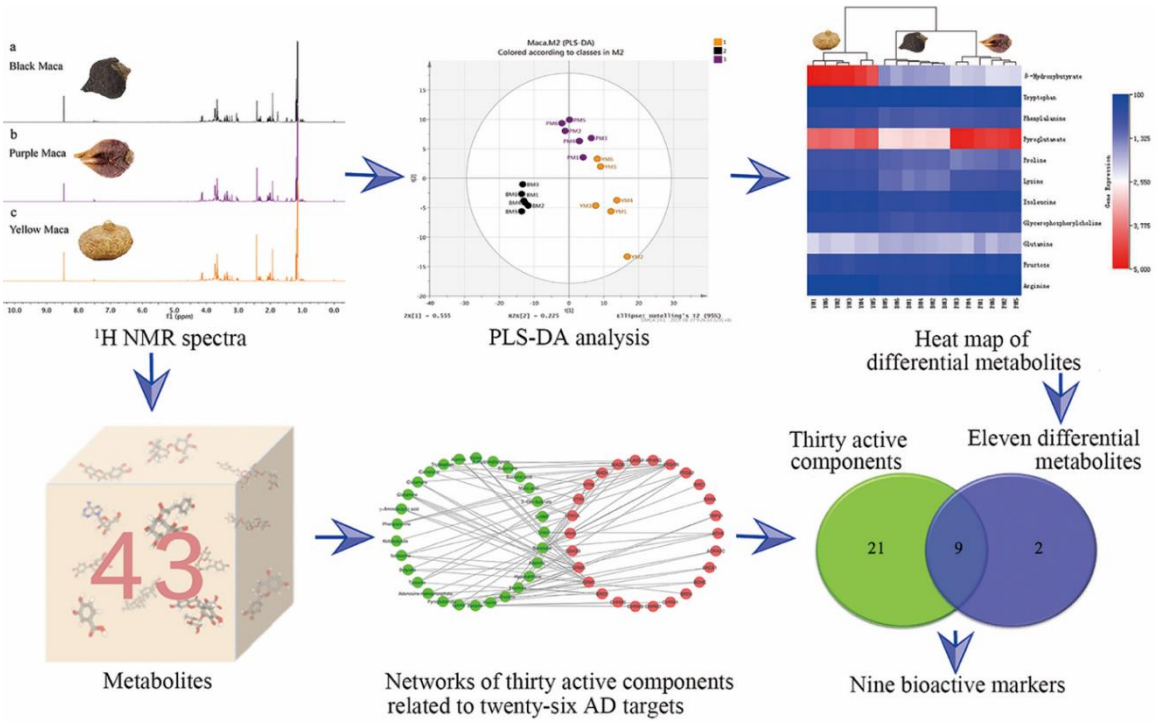

Fig. 1: Entire framework based on strategy integrating metabonomics and network pharmacology.

Results and Discussion

The bioactive markers of different maca color types from Yunnan, China, against Alzheimer's disease (AD) were investigated using a network construction approach with a network pharmacology model based on ^{1}H-NMR and multivariate data analysis (Fig. 1). All ingredients from Yunnan maca of three different colors were explored to build a compound library. Next, multivariate data analysis was used to screen differential metabolites. Potential targets and active compounds were then data-mined from network pharmacology. Subsequently, the acquired pharmacological data were integrated into the compound-target networks. Finally, the effects of every potentially active ingredient based on network-based efficacy weighted by intersection and the literature were discussed. Based on this analysis, the bioactive markers of different maca color types in Yunnan were explored.

Analysis of cell viability

Fig. 2 shows that L-glutamic acid can decrease the viability of SH-SY5Y cells. However, 5 mM L-glutamic acid, which resulted in relative cell viability of 54.1±1.45%, was selected to induce cell damage and evaluate the protective effects of different maca color types. Furthermore, treating the cells for 24 h with different doses of maca showed a significant effect on cultured SH-SY5Y cell viability. Three maca color types with doses of 2 mg/mL significantly inhibited L-glutamic acid-induced toxicity after 24 h and had a moderate effect at 1 mg/ml, but cell damage could not be prevented with a yellow maca dose of 0.5 mg/mL.

Metabolite identification by ^{1}H-NMR spectroscopy and multivariate data analysis

Typical ^{1}H-NMR spectra in Fig. 3 show the representative compositions of the upper layer of MeOH–H_2O mixture (1:2) extracting maca. Spectroscopic data were assigned to different metabolites based on compounds in the literature. The metabolites discovered were interpreted by analysis of the ^{1}H-NMR spectra and with an HMDB database (Fig. 4, Table-1). The chemical shifts (^{1}H) and coupling constants of metabolites found in maca were recorded, including amino acids, organic acids, lipids, and others [28]. Amino acids, including isoleucine (d 0.96, t, J = 6.6 Hz; 1.01, d, J = 7.2 Hz) [29-31], alanine (d 1.48, d, J = 7.2 Hz; 3.77, q, J = 7.2 Hz) [29-32], valine (d 0.99, d, J = 6.6 Hz; 1.04, d, J = 7.2 Hz; 3.58, s; 3.62, d) [29-33], lysine (d 3.04, t, J = 7.57 Hz) [30], glycine (d 3.55, s) [29], proline (d 2.00, m; 2.07, m; 2.35, m; 3.33, dt, J = 14.02, 7.10 Hz; 3.41, m; 4.12, dd, J = 8.63, 6.42 Hz) [31], tyrosine (d 6.89, d; 7.19, d; 3.15, dd; 3.94, dd) [30, 31], phenylalanine (d 3.29, dd; 7.33, d; 7.40, m; 7.44, m) [31], glutamate (d 2.06, m; 2.35, m) [29, 31], arginine (d 1.75, m; 3.76, t, J = 6.0 Hz) [31],

were evident in the spectra between d 0.96 and 7.55. Organic acids, including butyrate (d 0.90, t; 0.94, t, J = 8.87 Hz; 1.56, m; 2.16, t) [30], formic acid (d 8.46, s) [33], malic acid (d 2.69, dd, J = 15.6, 3.6 Hz; 4.29, dd, J = 9.0, 3.6 Hz) [33], lactate (d 1.33, d) [29-31], succinic acid (d 2.42, s) [31, 33], β-aminobutyric acid (d 1.91, m; 2.30, t; 3.02, t) [31], acetic acid (d 1.92, s) [33], pyruvate (d 2.23, s) [31], benzoate (d 7.48, t; 7.87, d) [31], were evident in the spectra between d 0.90 and 8.46. Others compounds, including glutamine (d 3.56, t) [29-31], uracil (d 5.80, d; 7.53, d) [29], adenine (d 8.29, s) [31], betaine (d 3.90, s) [29], carnosine (d 7.03, d; 7.05, s; 7.74, d) [31], hypoxanthine (d 8.19, s; 8.21, s) [31], adenosine monophosphate (d 4.37, m; 4.51, m; 8.61, s) [30], and acetamide (d 1.99, s) [31], were evident in the spectra between d 1.19 and 8.19.

Multivariate data analysis

Multivariate statistical analysis is an effective tool for analyzing and processing the observation data of multiple random variables, provides useful information on the interdependence, causality and relative importance of random variables, and can predict the value of variables. Because the object of multivariate statistical analysis is the original data itself, the information omission and change caused by the form transformation process are excluded, and the most original and objective information can be mined. Variable importance in projection analysis variable importance in projection (VIP) is an important indicator reflecting the explanatory ability of independent variables to dependent variables. The greater its value, the stronger the explanatory ability of the independent variable to dependent variables. When VIP is greater than 1, the independent variable has significant importance in explaining dependent variables, and these factors play a leading role in influencing the differential metabolites.

The multivariate statistical analysis was applied to tell the component differences among different maca color types. Aqueous methanol was subjected to PCA to display the similarities or differences among maca. Fig 5A shows clear separation among the different maca color types in the score plot of the four PCs (PC1: 56.0%; PC2: 23.4%), suggesting substantial chemical differences among them. PLS-DA was further explored in maca samples (Fig 5B). Parameters R2 (0.988) Q2 (0.968) and permutation tests (permutation number, 200) indicate the good fit and validity of the model (Fig 5C), and reveal high predictability and accuracy [34]. The maca metabolites with the variable importance in the projection (VIP) > 1 in the PLS-DA model were regarded as potential biomarkers. The corresponding results show that the metabolites distinguish of the different maca color types included arginine, lysine, isoleucine, phenylalanine, β-hydroxybutyrate, tryptophan, pyroglutamate, proline, glycerophosphorylcholine, glutamine, and fructose (Table 2).

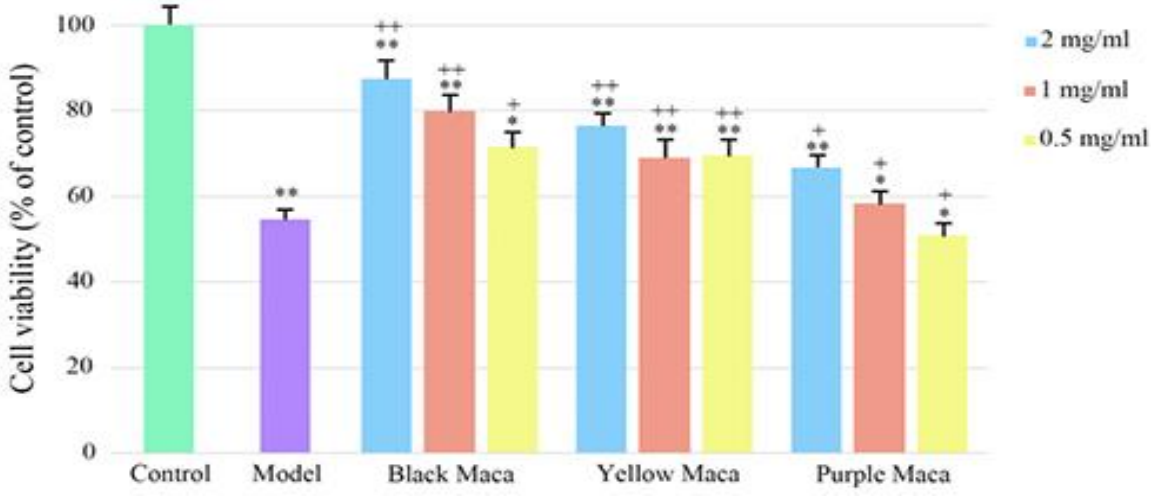

Fig. 2: Protective effects of different maca color types against L-glutamic acid-induced SH-SY5Y cell damage. Different maca concentrations were added 30 min before glutamate. Cells were treated with L-glutamic acid (5 mM) and different maca concentrations for 24 h. Data are expressed as mean ± SEM; n=6 wells for each group. *P < 0.05 and **P < 0.01 vs. control cells. +P < 0.05 and ++P < 0.01 vs. L-glutamic acid-treated cells.

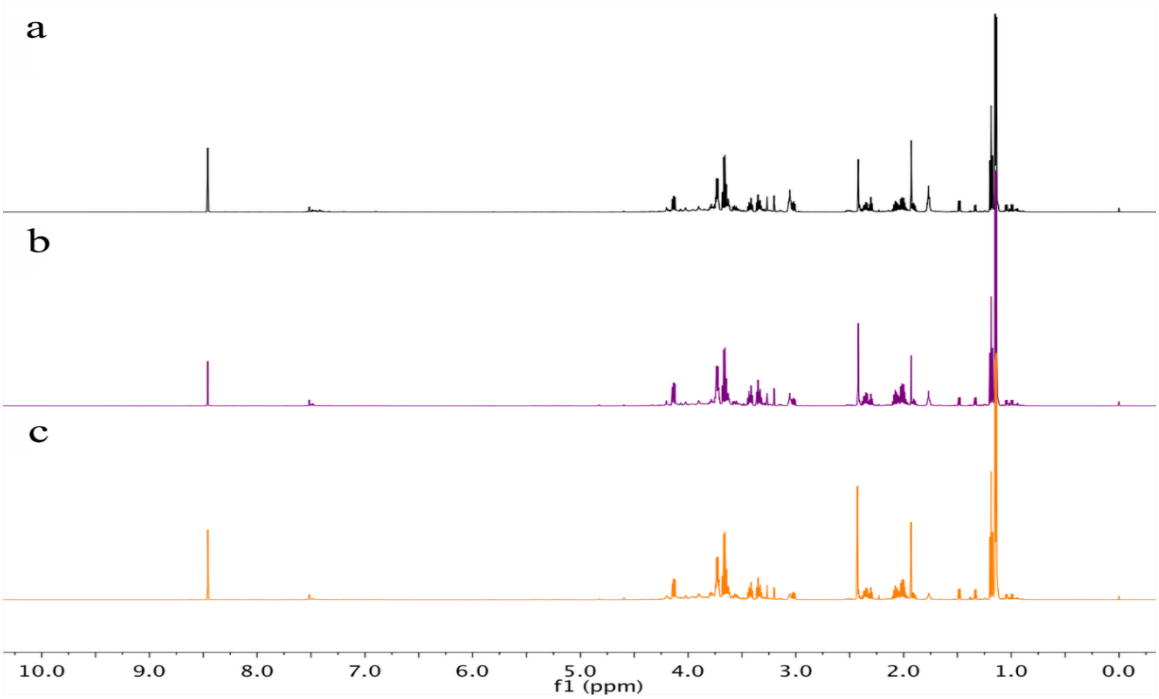

Fig. 3: Representative 600-MHz ^{1}H-NMR spectra (NMR solvent: NaH_2PO_4 buffer in D_2O) of aqueous methanol extracts from different maca color types in Yunnan. (a) Yunnan black maca, (b) purple maca, and (c) yellow maca.

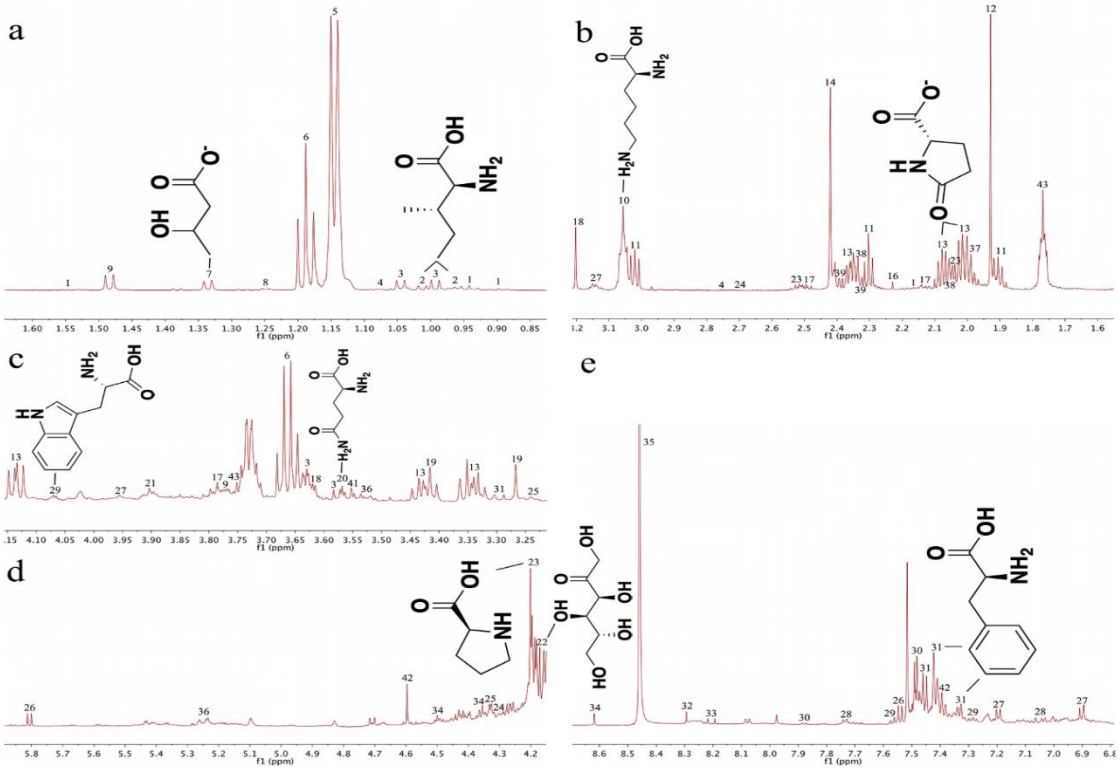

Fig. 4: ^{1}H-NMR fingerprint spectrum of maca: (a) d 0.85–1.60, (b) d 1.60–3.20, (c) d 3.25–4.15, (d) d 4.20–5.80, (e) d 6.80–8.60.

Table-1: ^{1}H-NMR assignments of major metabolites in maca.

No.	Metabolites	δ/ppm
1	Butyrate	0.90(t), 0.94(t, J=8.87Hz), 1.56(m), 2.16(t)
2	Isoleucine	0.96(t, 6.6), 1.01(d, 7.2)
3	Valine	0.99(d, J=6.6Hz), 1.04(d, J=7.2Hz), 3.58(s), 3.62(d)
4	Ketobutyrate	1.07(t), 2.75(s)
5	Isobutyrate	1.14(d)
6	Ethanol	1.19(t), 3.65(q)
7	β-Hydroxybutyrate	1.24(d)(J=6.6)
8	Lactate	1.33(d)
9	Alanine	1.48(d, J=7.2Hz), 3.77(q, J=7.2Hz)
10	Lysine	3.04(t, J=7.57Hz)
11	γ-Aminobutyric acid	1.91(m), 2.30(t), 3.02(t)
12	Acetic acid	1.92(s)
13	Proline	2.00(m), 2.07(m), 2.35(m), 3.33(dt, J=14.02, 7.10Hz), 3.41(m), 4.12(dd, J=8.63, 6.42Hz)
14	Succinic acid	2.42(s)
15	Succinate	2.40(s)
16	Pyruvate	2.23(s)
17	Glutamate	2.14(m), 2.50(m), 3.78(t, 6.8)
18	Phosphoryl-choline	3.22(s), 3.61(t, J=2.20Hz)
19	Taurine	3.26(s), 3.41(s)
20	Glutamine	3.56(t)
21	Betaine	3.90(s)
22	Fructose	4.16(d, J=8.0)
23	Pyroglutamate	2.04(m), 2.52(m), 4.18(dd, 3.6)
24	Malic acid	2.69(dd, J=15.6, 3.6Hz), 4.29(dd, J=9.0, 3.6Hz)
25	Glycerophosphorylcholine	3.23(s), 4.33(m)
26	Uracil	5.80(d), 7.53(d)
27	Tyrosine	6.89(d), 7.19(d), 3.15(dd), 3.94(dd)
28	Carnosine	7.03d, 7.05(s), 7.74(d)
29	Tryptophan	4.06(dd), 7.21(t), 7.28(t), 7.55(d)
30	Benzoate	7.48(t), 7.87(d)
31	Phenylalanine	3.29(dd), 7.33(d), 7.40(m), 7.44(m)
32	Adenine	8.29(s)
33	Hypoxanthine	8.19(s), 8.21(s)
34	Adenosine monophosphate	4.37(m), 4.51(m), 8.61(s)
35	Formic acid	8.46(s)
36	α-Glucose	3.53(dd), 5.23(dd)
37	Acetamide	1.99(s)
38	Glutamate	2.06(m), 2.35(m)
39	3-OH-butyrate	2.31(m), 2.41(m)
40	Pyruvate	2.38(s)
41	Glycine	3.55(s)
42	5-Hydroxymethyl Furfuraldehyde	7.38(d, J=3.6Hz), 4.61(s)
43	Arginine	1.76(m), 3.76(t, J=6.0)

Table-2: VIP values of major metabolites for the separation of Yunnan black maca, purple maca, and yellow maca samples in PLS-DA-derived score plots.

No.	Metabolites	δ/ppm	VIP	Fold changea	Trenda	Fold changeb	Trendb	Fold changec	Trendc
2	Isoleucine	1.01206	1.02	1.69E+00	↑**	1.13E+00	↑*	1.00E+00	*
7	β-Hydroxybutyrate	1.2515	1.25	3.53E-01	↓**	4.62E-01	↓**	1.00E+00	**
10	Lysine	3.04727	1.02	1.73E+00	↑**	1.14E+00	↑**	1.00E+00	**
13	Proline	2.00971	1.56	1.52E+00	↑**	1.49E+00	↑**	1.00E+00	**
19	Phenylalanine	3.28671	1.06	1.52E+00	↑**	1.33E+00	↑**	1.00E+00	**
20	Glutamine	3.80549	1.03	8.84E-01	↓**	8.87E-01	↓**	1.00E+00	**
22	Fructose	4.20455	1.48	8.42E-01	↓*	6.55E-01	↓**	1.00E+00	*
23	Pyroglutamate	2.04962	1.35	7.27E-01	↓**	1.16E+00	↑**	1.00E+00	**
25	Glycerophosphorylcholine	3.2468	1.05	1.47E+00	↑**	1.30E+00	↑**	1.00E+00	**
29	Tryptophan	7.55666	1.22	9.27E-01	↓*	1.12E+00	↑*	1.00E+00	*
43	Arginine	1.77028	1.01	3.41E+00	↑**	1.39E+00	↑**	1.00E+00	**

a,b,c "↑" and "↓" represent up-regulation and down-regulation of compounds, respectively, in black maca and purple maca groups compared with the Yunnan yellow maca group. **P < 0.01; *P < 0.05.

Systematic investigation of AD effect mechanism

^{1}H-NMR analysis of maca showed a total of 43 metabolites. Of these, 26 targets corresponding to 30 metabolites were determined to be associated with AD. Network nodes indicate metabolites and protein targets (**Fig** 6). According to network statistics, the average node degree was 2.7, with the PTGFR hub showing the highest degree of 11, followed by GRM and ACHE hubs with 10 and 4, respectively. These hubs, particularly PTGFR, GRM, ACHE, HTR1A, and PTGS2, have already been described to be involved in AD [35-39]. Furthermore, the intersection of 30 active components and eleven differential metabolites resulted in nine bioactive markers related to AD, including lysine, isoleucine, phenylalanine, β-hydroxybutyrate, tryptophan, pyroglutamate, proline, glutamine, and fructose (Fig. 7). Studies have shown that acetylcholinesterase (AChE) increases amyloid fibril assemble triggering AD [40]. The large presence of neurotoxic Aβ species in human AD tissues and disease

models derives from the aggregation of pyroglutamate-modified Aβ peptides [41]. Phenylalanine prevents damage to brain AChE by •OH radicals and, therefore, is potentially useful for preventing certain cholinergic neural dysfunctions [42]. Proline inhibits acetylcholinesterase activity through oxidative stress [43]. PTGS2, a susceptibility gene in arachidonic acid metabolism, may be involved in the pathogenesis of AD [37]. Alterations in glutamatergic neurotransmission and glutamate-glutamine cycle are major players in the propagation of neuronal destruction and contribute to altered AD pathology [44]. The amino acid pyroglutamate acid and its derivatives in the human brain and spinal fluid are masters of communication and contain a key brain chemical that enhances memory and mental function [45]. Maca is rich in proteins and amino acids, especially branched-chain amino acids which are related to the antifatigue effect [46]. In both sexes, β-aminobutyric acid stimulates gonadotropin secretion. And the steroidal environment is an important regulator of β-aminobutyric acid action [47]. The above results showed that nine bioactive markers played an important role in AD treatment, with the above bioactive markers suggested to be the material basis of the traditional efficacy of Yunnan maca.

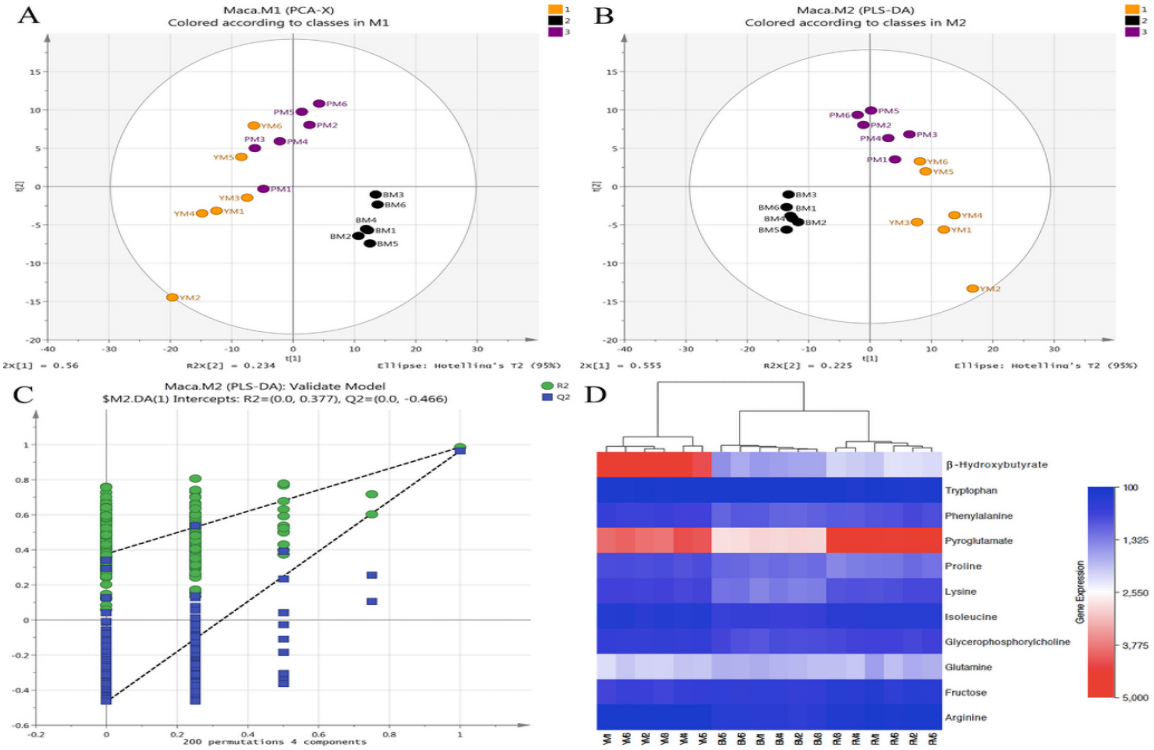

Fig. 5: (A) PCA scores plots, (B) PLS-DA scores plots, (C) permutation and (D) heatmap of differential metabolites among Yunnan black maca (—.), purple maca (—.), and yellow maca (—.).

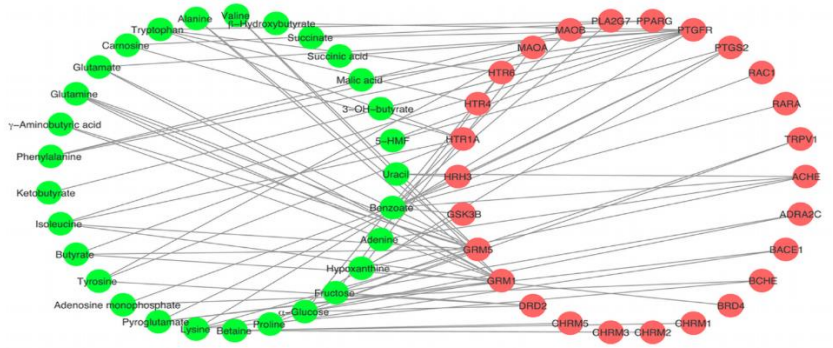

Fig. 6: Metabolites and target networks of three maca colors in Yunnan.

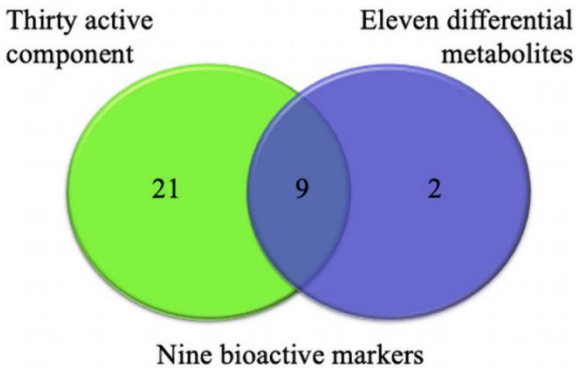

Fig. 7: Venn diagram of potential active compounds and differential metabolites among three maca colors in Yunnan.

Conclusions

The chemical components in different maca color types from Yunnan province, China, were compared using ^{1}H-NMR-based metabolite fingerprinting. The results proved that ^{1}H-NMR is an effective tool for determining the metabolic composition of complex mixtures. Multivariate data analysis identified 11 differential metabolites and significantly distinguished the different maca color types. Network pharmacological results showed that 30 active components from maca were related to traditional efficacy against AD. Furthermore, the intersection of 11 differential metabolites and 30 active components resulted in nine bioactive markers related to both the identification of maca and AD individually, including lysine, isoleucine, phenylalanine, β-hydroxybutyrate, tryptophan, pyroglutamate, proline, glutamine, and fructose. Therefore, the above nine bioactive markers were used for the quality evaluation of commercial products derived from different maca color types from Yunnan province, China. The roles of secondary metabolites in distinguishing the different maca color types should be further investigated.

Author Contribution Statement

All experiments were designed by Jiaming Sun. Jingwei Lv and Chunnan Li performed the experiments. Jingwei Lv analyzed the data and wrote the paper. Xiaochen Gao contributed samples. Nanxi Zhang, Kaiyue Zhang and Na Li done the literature search and drafted the manuscript. Lingwen Meng, Yinping Yang and Hui Zhang edited the manuscript. All authors reviewed the final manuscript.

Funding

This research was funded by the grants from the Science and Technology Development Project of Jilin Province (No. 20200404081YY), National Natural Science Foundation of China (No. 31570347), Science and Technology funds of Administration of Traditional Chinese Medicine of Jilin Province (No. 2022011, 2020195).

Reference

1. M. Hao, D. Ji, L. Li, L. Su, W. Gu, L. Gu, Q. Wang, T. Lu, C. Mao, Mechanism of Curcuma wenyujin Rhizoma on Acute Blood Stasis in Rats Based on a UPLC-Q/TOF-MS Metabolomics and Network Approach, *Molecules (Basel, Switzerland)*, **24**, (2018).
2. J. J. Chen, Q.S. Zhao, Y.L. Liu, S.H. Zha, B. Zhao, Identification of maca (Lepidium meyenii Walp.) and its adulterants by a DNA-barcoding approach based on the ITS sequence, *Chin. J. Nat. Med.*, **13**, 653 (2015).
3. Y. Wang, Y. Wang, B. McNeil, L.M. Harvey, Maca: An Andean crop with multi-pharmacological functions, *Food Res. Int*., **40**, 783 (2007).
4. E.H. Choi, J.I. Kang, J.Y. Cho, S.H. Lee, T.S. Kim, I.H. Yeo, H.S. Chun, Supplementation of standardized lipid-soluble extract from maca (Lepidium meyenii) increases swimming endurance capacity in rats, *J. Funct. Foods*, **4** , 568 (2012).
5. M.E. Cordova-Ruiz, Effect of Maca (Lepidium meyenii Walp) in Cognitive Functions in an Experimental Animal Model, *Neuroimmunomodulation*, **18**, 369 (2011).
6. H. Liu, W. Jin, C. Fu, P. Dai, Y. Yu, Q. Huo, L. Yu, Discovering anti-osteoporosis constituents of maca (Lepidium meyenii) by combined virtual screening and activity verification, *Food Res. Int.*, **77**, 215 (2015).
7. Y. Zou, W. Aboshora, J. Li, T. Xiao, L. Zhang, Protective Effects of Lepidium meyenii (Maca) Aqueous Extract and Lycopene on Testosterone

Propionate-Induced Prostatic Hyperplasia in Mice, *Phytother. Res.*, **31**, 1192 (2017).
8. D. Nuñez, P. Olavegoya, G.F. Gonzales, C. Gonzales-Castañeda, Red Maca (Lepidium meyenii), a Plant from the Peruvian Highlands, Promotes Skin Wound Healing at Sea Level and at High Altitude in Adult Male Mice, *High Alt. Med. Biol.*, **18**, 372 (2017).
9. C.H. Ran, D. Shin, M.J. Lee, S.J. Lee, H.J. Park, , J.-Y. Song, , I.S. Kim, Effect of Lepidium spp. (Maca) Extract on the Improvement of Sexual Function inRats Induced Erectile Dysfunction with Ethanol, *J. Korean Soc. Food Sci. Nutr.*, **31**, 328 (2018).
10. H.O. Meissner, L. Xu, W. Wan, F. Yi, Glucosinolates profiles in Maca phenotypes cultivated in Peru and China (Lepidium peruvianum syn. L. meyenii), *Phytochem. Lett.*, **31**, 208 (2019).
11. D. Kasprzak, B. Jodlowska-Jedrych, K. Borowska, A. Wojtowicz, Lepidium meyenii (Maca)–multidirectional health effects–review, *Curr. Issues Pharm. Med. Sci.*, **31**, 107 (2018).
12. Y. Tang, Z.-Y. Zhu, L.-C. Pan, H. Sun, Q.-Y. Song, Y. Zhang, Structure analysis and anti-fatigue activity of a polysaccharide from Lepidium meyenii Walp, *Nat. Prod. Res.*, **33**, 2480 (2019).
13. Y. Zheng, W.C. Zhang, Z.Y. Wu, C.X. Fu, A.L. Hui, H. Gao, P.P. Chen, B. Du, H.W. Zhang, Two macamide extracts relieve physical fatigue by attenuating muscle damage in mice, *J. Sci. Food Agric.*, **99**, 1405 (2019).
14. N. Bai, K. He, M. Roller, C.-S. Lai, L. Bai, M.-H. Pan, Flavonolignans and other constituents from Lepidium meyenii with activities in anti-inflammation and human cancer cell lines, *J. Agric. Food Chem.*, **63**, 2458 (2015).
15. I. Muhammad, J. Zhao, I.A. Khan, Maca (Lepidium meyenii), *Encyclopedia of Dietary Supplement, 2nd ed.*; Coates, P., Blackman, MR, Cragg, G., Levine, M., Moss, J., White, J., Eds, 522 (2005).
16. Z. Ai, A.-F. Cheng, Y.-T. Yu, L.-J. Yu, W. Jin, Antidepressant-like behavioral, anatomical, and biochemical effects of petroleum ether extract from maca (Lepidium meyenii) in mice exposed to chronic unpredic**table** mild stress, *J. Med. Food*, **17**, 535 (2014).
17. F. Uchiyama, T. Jikyo, R. Takeda, M. Ogata, Lepidium meyenii (Maca) enhances the serum levels of luteinising hormone in female rats, *J. Ethnopharmacol.*, **151**, 897 (2014).
18. F.E. Chain, A. Grau, J.C. Martins, C.A. Catalán, Macamides from wild 'maca', Lepidium meyenii Walpers (Brassicaceae), *Phytochem. Lett.*, **8**, 145 (2014).
19. G. Li, U. Ammermann, C.F. Quirós, Glucosinolate contents in maca (Lepidium peruvianum Chacon) seeds, sprouts, mature plants and several derived commercial products, *Econ. Bot.*, **55**, 255 (2001).
20. S. Wang, F. Zhu, Chemical composition and health effects of maca (Lepidium meyenii), *Food chemistry*, **288**, 422 (2019).
21. H. Tang, Y. Wang, Metabonomics: a revolution in progress, *Sheng wu hua xue yu sheng wu wu li jin zhan*, **33**, 401 (2006).
22. Q. Song, A.-h. Zhang, G.-l. Yan, L. Liu, X.-j. Wang, Technological advances in current metabolomics and its application in tradition Chinese medicine, *RSC Adv.*, **7**, 53516 (2017).
23. A.L. Hopkins, Network pharmacology: the next paradigm in drug discovery, *Nat. Chem. Biol.*, **4**, 682 (2008).
24. J. Zhao, B. Avula, M. Chan, C. Clément, M. Kreuzer, I.A. Khan, Metabolomic differentiation of maca (Lepidium meyenii) accessions cultivated under different conditions using NMR and chemometric analysis, *Planta Med.*, **78**, 90 (2012).
25. R. Consonni, L.R. Cagliani, The potentiality of NMR-based metabolomics in food science and food authentication assessment, *Magn. Reson. Chem.*, (2019).
26. J. Gao, V.G. Tarcea, A. Karnovsky, B.R. Mirel, T.E. Weymouth, C.W. Beecher, J.D. Cavalcoli, B.D. Athey, G.S. Omenn, C.F. Burant, H.V. Jagadish, Metscape: a Cytoscape plug-in for visualizing and interpreting metabolomic data in the context of human metabolic networks, *Bioinformatics*, **26**, 971 (2010).
27. M.E. Smoot, K. Ono, J. Ruscheinski, P.-L. Wang, T. Ideker, Cytoscape 2.8: new features for data integration and network visualization, *Bioinformatics*, **27**, 431 (2010).
28. A. Marseglia, D. Acquotti, R. Consonni, L.R. Cagliani, G. Palla, A. Caligiani, HR MAS (1)H-NMR and chemometrics as useful tool to assess the geographical origin of cocoa beans - Comparison with HR (1)H-NMR, *Food Res. Int.*, **85**, 273 (2016).
29. L. Jiang, Z.H. Si, M.H. Li, H. Zhao, Y.H. Fu, Y.X. Xing, W. Hong, L.Y. Ruan, P.M. Li, J.S. Wang, (1)H-NMR-based metabolomics study of liver damage induced by ginkgolic acid (15:1) in mice, *J Pharm Biomed Anal*, **136**, 44 (2017).
30. Y. Zhao, H. Chen, J. Feng, Z. Chen, S. Cai, (1)H-NMR-based compositional identification of different powdered infant formulas, *Food chemistry*, **230**, 164 (2017).

31. W. Kexin, G. Li, Z. Yuzhi, Q. Xuemei, D. Guanhua, 1H-NMR-based metabolomics study on antiproliferative effect of matrine in human hepatoma cells, *J Chinese Traditional and Herbal Drugs*, **48**, 4275 (2017).
32. Y. Yuan, Y. Zhao, J. Yang, Y. Jiang, F. Lu, Y. Jia, B. Yang, Metabolomic analyses of banana during postharvest senescence by (1)H-high resolution-NMR, *Food chemistry*, **218**, 406 (2017).
33. G. Papotti, D. Bertelli, R. Graziosi, A. Maietti, P. Tedeschi, A. Marchetti, M.J.L.-F.S. Plessi, Technology, Traditional balsamic vinegar and balsamic vinegar of Modena analyzed by nuclear magnetic resonance spectroscopy coupled with multivariate data analysis, *LWT Food Sci. Technol.*, **60**, 1017 (2015).
34. Z. Zhang, Y. Zhang, C. Liu, M. Zhao, Y. Yang, H. Wu, H. Zhang, H. Lin, L. Zheng, H. Jiang, Serum Metabolomic Profiling Identifies Characterization of Non-Obstructive Azoospermic Men, *Int J Mol Sci*, **18**, (2017).
35. A. P. Murray, M.B. Faraoni, M.J. Castro, N.P. Alza, V. Cavallaro, Natural AChE inhibitors from plants and their contribution to Alzheimer's disease therapy, *Curr. Neuropharmacol.*, **11**, 388 (2013).
36. F.J. Carvajal, N.C. Inestrosa, Interactions of AChE with Aβ aggregates in Alzheimer's brain: therapeutic relevance of IDN 5706, *Front. Mol. Neurosci.*, **4**, 19 (2011).
37. S. L. Ma, N.L.S. Tang, Y.P. Zhang, L.-d. Ji, C.W.C. Tam, V.W.C. Lui, H.F.K. Chiu, L.C.W. Lam, Association of prostaglandin-endoperoxide synthase 2 (PTGS2) polymorphisms and Alzheimer's disease in Chinese, *Neurobiol. Aging*, **29**, 856 (2008).
38. Q. Chen, B. Liang, Z. Wang, X. Cheng, Y. Huang, Y. Liu, Z. Huang, Influence of four polymorphisms in ABCA1 and PTGS2 genes on risk of Alzheimer's disease: a meta-analysis, *J. Neurol. Sci.*, **37**, 1209 (2016).
39. B. Tang, C. Capitao, B. Dean, E.A. Thomas, Differential age-and disease-related effects on the expression of genes related to the arachidonic acid signaling pathway in schizophrenia, *Psychiatry Res.*, **196**, 201 (2012).
40. V.N. Talesa, Acetylcholinesterase in Alzheimer's disease, *Mech. Ageing Dev.*, **122**, 1961 (2001).
41. A. Tarditi, A. Caricasole, G. Terstappen, Therapeutic targets for Alzheimer's disease, *Expert Opin. Ther. Targets*, **13**, 551 (2009).
42. S. Tsakiris, P. Angelogianni, K.H. Schulpis, J.C. Stavridis, Protective effect of L-phenylalanine on rat brain acetylcholinesterase inhibition induced by free radicals, *Clin. Biochem.*, **33**, 103 (2000).
43. D. Delwing, F. Chiarani, D. Delwing, C.S. Bavaresco, C.M. Wannmacher, M. Wajner, A.T. Wyse, Proline reduces acetylcholinesterase activity in cerebral cortex of rats, *Metab. Brain Dis.*, **18** , 79-86 (2003).
44. H.S. Walton, P.R. Dodd, Glutamate–glutamine cycling in Alzheimer's disease, *Neurochem. Int.*, **50**, 1052 (2007).
45. C.P. Sullivan, E.A. Berg, R. Elliott-Bryant, J.B. Fishman, A.C. McKee, P.J. Morin, M.A. Shia, R.E. Fine, Pyroglutamate-Aβ 3 and 11 colocalize in amyloid plaques in Alzheimer's disease cerebral cortex with pyroglutamate-Aβ 11 forming the central core, *Neurosci. Lett.*, **505**, 109 (2011).
46. J. Li, L. Chen, J. Li, Z. Duan, S. Zhu, L. Fan, The Composition analysis of Maca (Lepidium meyenii Walp.) from xinjiang and its antifatigue activity, *J. Food Qual.*, **2017**, (2017).
47. E.L. Mañanos, I. Anglade, J. Chyb, C. Saligaut, B. Breton, O. Kah, Involvement of γ-aminobutyric acid in the control of GtH-1 and GtH-2 secretion in male and female rainbow trout, *Neuroendocrinology*, **69**, 269 (1999).